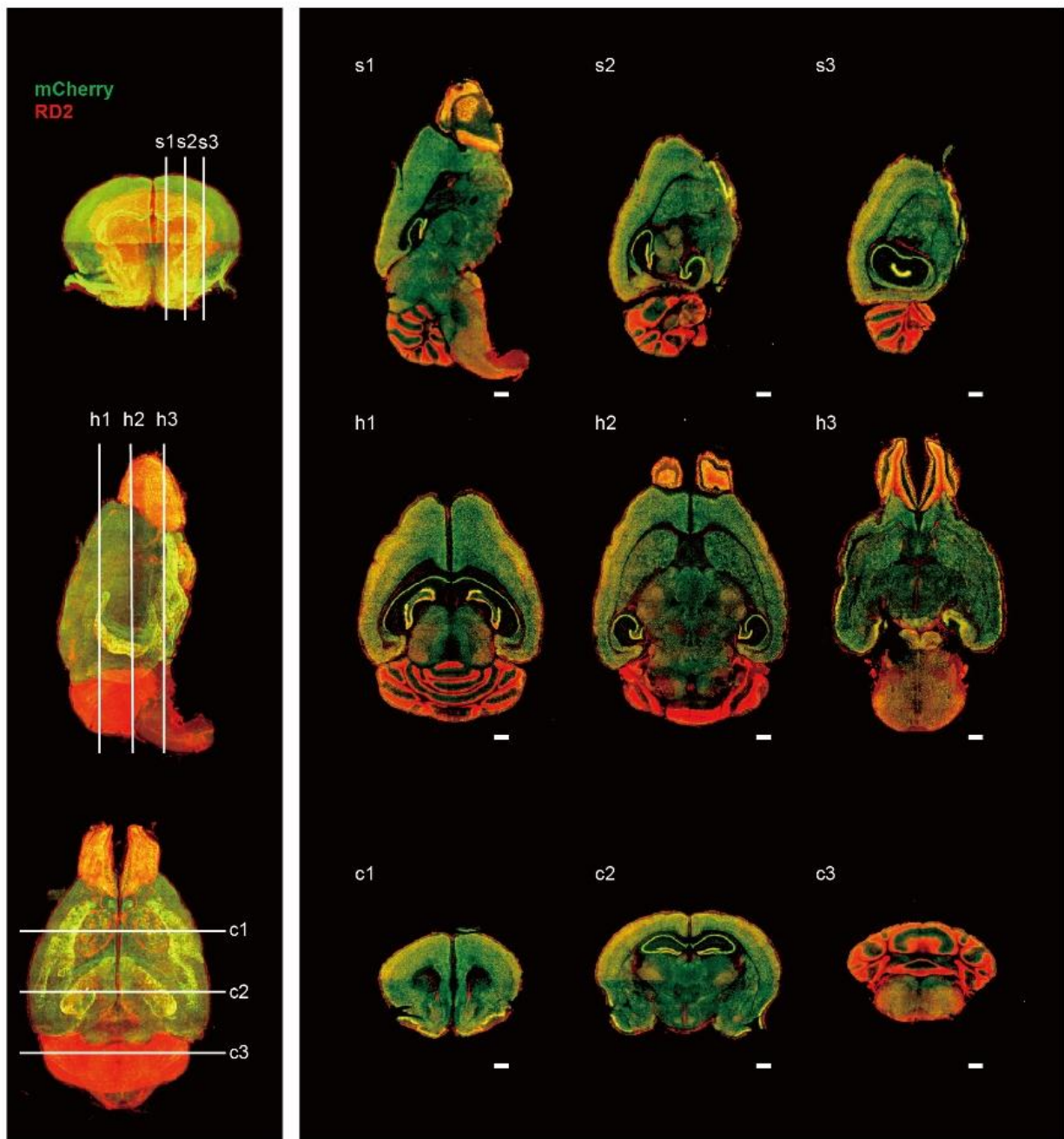


In the format provided by the authors and unedited.

Advanced CUBIC tissue clearing for whole-organ cell profiling

Katsuhiko Matsumoto^{1,10}, Tomoki T. Mitani^{1,2,3,10}, Shuhei A. Horiguchi^{1,4,10}, Junichi Kaneshiro⁵, Tatsuya C. Murakami⁶, Tomoyuki Mano^{7,8}, Hiroshi Fujishima¹, Ayumu Konno⁹, Tomonobu M. Watanabe⁵, Hirokazu Hirai⁹ and Hiroki R. Ueda^{1,6,7,8*}

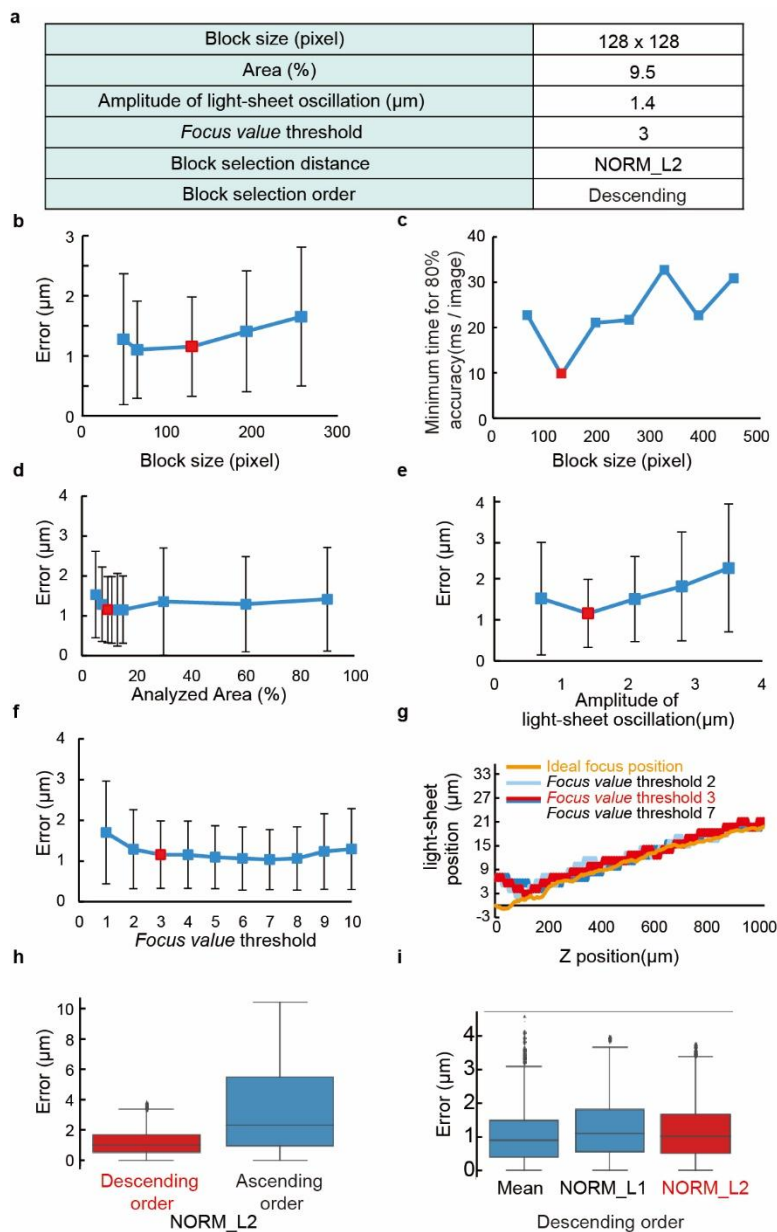
¹Laboratory for Synthetic Biology, RIKEN Center for Biosystems Dynamics Research, Osaka, Japan. ²Faculty of Medicine, Osaka University, Osaka, Japan. ³Osaka University Hospital, Osaka, Japan. ⁴Department of Electrical Engineering and Information Systems, Graduate School of Engineering, The University of Tokyo, Tokyo, Japan. ⁵Laboratory for Comprehensive Bioimaging, RIKEN Center for Biosystems Dynamics Research, Osaka, Japan. ⁶Department of Systems Pharmacology, Graduate School of Medicine, The University of Tokyo, Tokyo, Japan. ⁷Department of Information Physics and Computing, Graduate School of Information Science and Technology, The University of Tokyo, Tokyo, Japan. ⁸International Research Center for Neurointelligence (WPI-IRCN), UTIAS, The University of Tokyo, Tokyo, Japan. ⁹Department of Neurophysiology & Neural Repair, Gunma University Graduate School of Medicine, Maebashi, Japan. ¹⁰These authors contributed equally: Katsuhiko Matsumoto, Tomoki T. Mitani, Shuhei A. Horiguchi. *e-mail: uedah-tky@umin.ac.jp



Supplementary Figure 1

3D and cross section images of CUBIC-L/R+ treated brain.

Volume-rendered and cross-section images of CUBIC-L/R+ treated whole mouse brain labelled with H2B-mCherry (green) and RD2 (red). Overlapped signals are shown in yellow. Scale bar, 1mm. All experiments followed governmental and institutional guidelines for the animal experiments.

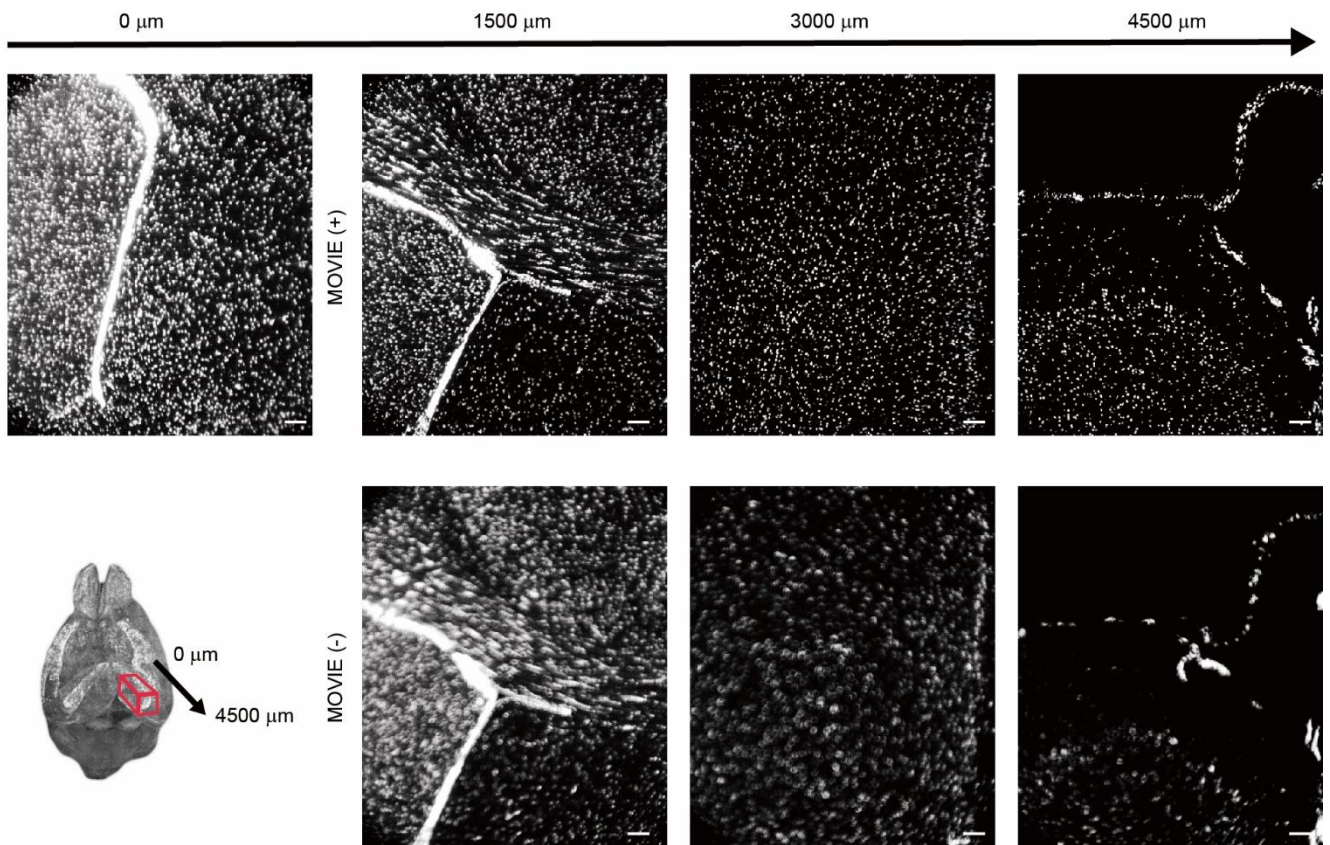


Supplementary Figure2

Parameter optimization for MOVIE-focus.

(a) Optimized six parameters of MOVIE-focus is shown in this table by comprehensive autofocus simulation by using 400,000 images data sets (400 of different light-sheet positions at every $0.35 \mu\text{m}$) which was acquired by our LSM at the $5 \mu\text{m}$ step size covering $5000 \mu\text{m}$ depth, using a PI stained mouse brain. Several parts of parameter optimization are shown as an example in (b)-(i). In these panels, only one or two parameters from six parameters are changed. (b) The relationship between block size for image analysis and mean error from ideal focus positions. Error bars show standard deviation of error. (c) The relationship among the block size for image analysis of MOVIE-focus and minimum calculation time for 80% focus accuracy. The focus accuracy was calculated from the ideal focus position, which is determined by the light-sheet position with the highest DCTS score. Although block size 128×128 and 64×64

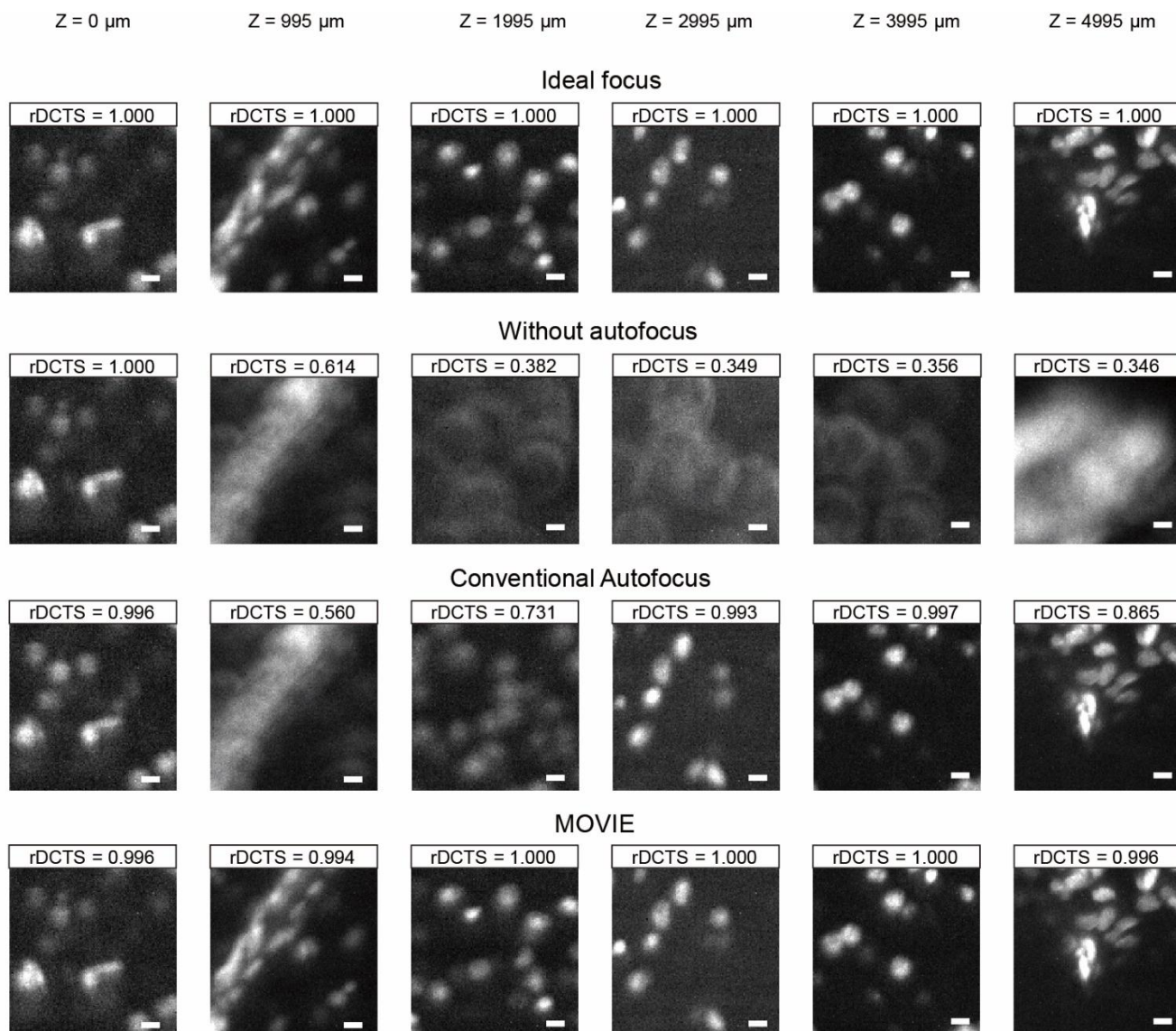
exhibit similar error in panel (b), the minimum calculation time of block size 128x128 is less than 10 ms per image and faster than that of block size 64x64. (d) The relationship between analyzed area and mean error from ideal focus positions. Error bars show standard deviation of error. (e) The relationship between amplitude of light-sheet oscillation and mean error from ideal focus positions. Error bars show standard deviation of error. (f) The relationship between focus value threshold and mean error from ideal focus positions. Error bars show standard deviation of error. (g) The relationship between focus value threshold and tracking ability. (h) The relationship between block selection order and mean error from ideal focus positions. "Descending" and "Ascending" indicate block selections from top or bottom, respectively. Error bars show standard deviation of error. (i) The relationship between block selection distance (distance function used in block selection; Mean, L^1 -norm and L^2 -norm) and mean error from ideal focus positions. Error bars show standard deviation of error.



Supplementary Figure 3

Result of autofocus simulation for MOVIE performance.

MOVIE-focus was simulated by 400,000 images data sets (400 of different light-sheet positions with $0.35\ \mu\text{m}$ span) which was acquired by our LSFM at the $5\ \mu\text{m}$ step size covering $5000\ \mu\text{m}$ depth, using a PI stained mouse brain. MOVIE (-) used the constant light-sheet position throughout. MOVIE (+) used parameters of **Figure S2a**. Scale bar, $100\ \mu\text{m}$.



Supplementary Figure 4

Result of autofocus simulation for four algorithms.

Result of autofocus simulation. 400,000 images data sets (400 of different light-sheet positions with 0.35 μm span) which was acquired by our LSM at the 5 μm step size covering 5000 μm depth were used. MOVIE used parameters optimized in **Figure S2a**. “Without autofocus” means the constant light-sheet position throughout. “Conventional Autofocus” was stop and exposure autofocus mode updated every 1000 μm . An ideal focus position was determined by the light-sheet position with the highest DCTS score of 400 images at each z position. rDCTS (relative DCTS) was calculated with division by DCTS of ideal focus positions. Scale bar, 10 μm .